ELSEVIER

Nuclear Physics B (Proc. Suppl.) 123 (2003) 177–185

NUCLEAR PHYSICS B PROCEEDINGS SUPPLEMENTS

www.elsevier.com/locate/npe

Measurement of hadronic cross section and preliminary results on the pion form factor using the radiative return at DAΦNE

The KLOE Collaboration *
presented by G. Venanzoni [a]

[a]Università and Sezione INFN Pisa

In the fixed energy environment of the e^+e^- collider DAΦNE, KLOE can measure the cross section of the process $e^+e^- \to$ hadrons as a function of the hadronic system energy using the radiative return. At energies below 1 GeV, $e^+e^- \to \rho \to \pi^+\pi^-$ is the dominating hadronic process. We report here on the status of the analysis for the $e^+e^- \to \pi^+\pi^-\gamma$ channel, which allows to obtain a preliminary measurement of the pion form factor using an integrated luminosity of $\sim 73\,pb^{-1}$.

1. Measuring the hadronic cross section with the KLOE detector

1.1. Motivation

The measurement of the hadronic cross section at low energy is of great importance for the improvement of the theoretical error of the anomalous magnetic moment of the muon, $a_\mu = (g_\mu - 2)/2$. The hadronic contribution a_μ^{hadr} is given by the hadronic vacuum polarization and cannot be calculated at low energy in the framework of perturbative QCD. Following a phenomenological approach, the hadronic contribution can however be evaluated from the measurement of R through a dispersion relation.

$$a_\mu^{hadr} = (\frac{\alpha m_\mu}{3\pi})^2 \int_{4m_\pi^2}^{\infty} ds \frac{R(s)\hat{K}(s)}{s^2}, \qquad (1)$$

where $R(s) = \frac{\sigma(e^+e^- \to hadrons)}{\frac{4\pi\alpha^2(s)}{3s}}$ and the kernel $\hat{K}(s)$ is a smooth bounded function growing from 0.63 at threshold to 1 at ∞. Due to the $1/s^2$ dependence in the integral, hadronic data at low energies are strongly enhanced in the contribution to a_μ^{hadr}. The error of the hadronic contribution is therefore given by the limited knowledge of hadronic cross section data. This error is the dominating contribution to the total error of a_μ^{theo} ($\delta a_\mu^{theo} \approx \delta a_\mu^{hadr}$) [1]

The discrepancy between the theoretical calculation [1,2,3,4], and the recent experimental value of a_μ [5] depends if τ data are used or not in the evaluation of a_μ^{had} [6,7]; a recent re-evaluation of the hadronic contribution to a_μ [8] found: $a_\mu^{theo} - a_\mu^{exp} = (33.9 \pm 11.2) \times 10^{-10}$ [e^+e^- *based*], $a_\mu^{theo} - a_\mu^{exp} = (16.7 \pm 10.7) \times 10^{-10}$ [τ *based*], corresponding to 3.0 and 1.6 standard deviations respectively, reflecting also a $1.6\,\sigma$ discrepancy between e^+e^- and τ evaluations of a_μ^{had}. A discus-

*The KLOE Collaboration: A. Aloisio, F. Ambrosino, A. Antonelli, M. Antonelli, C. Bacci, G. Bencivenni, S. Bertolucci, C. Bini, C. Bloise, V. Bocci, F. Bossi, P. Branchini, S. A. Bulychjov, R. Caloi, P. Campana, G. Capon, G. Carboni, M. Casarsa, V. Casavola, G. Cataldi, F. Ceradini, F. Cervelli, F. Cevenini, G. Chiefari, P. Ciambrone, S. Conetti, E. De Lucia, G. De Robertis, P. De Simone, G. De Zorzi, S. Dell'Agnello, A. Denig, A. Di Domenico, C. Di Donato, S. Di Falco, A. Doria, M. Dreucci, O. Erriquez, A. Farilla, G. Felici, A. Ferrari, M. L. Ferrer, G. Finocchiaro, C. Forti, A. Franceschi, P. Franzini, C. Gatti, P. Gauzzi, S. Giovannella, E. Gorini, F. Grancagnolo, E. Graziani, S. W. Han, M. Incagli, L. Ingrosso, W. Kluge, C. Kuo, V. Kulikov, F. Lacava, G. Lanfranchi, J. Lee-Franzini, D. Leone, F. Lu, M. Martemianov, M. Matsyuk, W. Mei, L. Merola, R. Messi, S. Miscetti, M. Moulson, S. Müller, F. Murtas, M. Napolitano, A. Nedosekin, F. Nguyen, M. Palutan, L. Paoluzi, E. Pasqualucci, L. Passalacqua, A. Passeri, V. Patera, E. Petrolo, L. Pontecorvo, M. Primavera, F. Ruggieri, P. Santangelo, E. Santovetti, G. Saracino, R. D. Schamberger, B. Sciascia, A. Sciubba, F. Scuri, I. Sfiligoi, T. Spadaro, E. Spiriti, G. L. Tong, L. Tortora, E. Valente, P. Valente, B. Valeriani, G. Venanzoni, S. Veneziano, A. Ventura, G. Xu, G. W. Yu.

0920-5632/03/$ – see front matter
doi:10.1016/S0920-5632(03)02176-5

sion on this subject can also be found in [9].

This unclear situation makes a precise measurement of the hadronic cross section at low energy mandatory, particularly in the channel $e^+e^- \to \rho \to \pi^+\pi^-$, which is the main ingredient for a_μ^{had}. Such a cross section has been already measured by the CMD-2 collaboration with an energy scan in the range below 1.4 GeV [10]; an accuracy of 0.6% was recently achieved in the region between 0.61 and 0.96 GeV [11].

1.2. Radiative Return

DAΦNE [12] is an e^+e^- storage-ring collider working at the ϕ resonance (1020 MeV). As an experiment at a collider with a fixed centre of mass energy, KLOE can measure the hadronic cross section $\sigma(e^+e^- \to \text{hadrons})$ as a function of the hadronic system energy using the *radiative return* [13,14] i. e. studying the process $e^+e^- \to$ hadrons+γ. The emission of one photon before the beams interact (Initial State Radiation, ISR in the following) lowers the interaction energy and makes possible to produce the hadronic system with an invariant mass varying from the ϕ mass down to the production threshold.

The method represents an alternative approach to the conventional energy scan used so far for hadronic cross section measurements. A very solid theoretical understanding of Initial State Radiation (described by the radiation function H) is mandatory in order to extract the cross section $\sigma(e^+e^- \to \text{hadrons})$ as a function of Q^2_{had} from the measured differential cross section $d\sigma(e^+e^- \to \text{hadrons}+\gamma)/dQ^2_{had}$:

$$Q^2_{had} \cdot \frac{d\sigma(e^+e^- \to \text{hadrons} + \gamma)}{dQ^2_{had}} = \sigma(e^+e^- \to \text{hadrons}) \cdot H(Q^2_{had}, \theta_\gamma)$$

where Q^2_{had} and θ_γ are respectively the invariant mass squared of the hadronic system and the acceptance cut on the polar angle of the photon.

Radiative corrections for $e^+e^- \to \pi^+\pi^-\gamma$, have been calculated up to ISR NLO by different theoretical groups [15,16,17,18,19,20], and recently implemented in a new Monte Carlo generator named PHOKHARA [21,22], This generator with a claimed accuracy of 0.5% has been used in the present analysis.

We want to stress that the radiative return has the merit compared with the conventional energy scan that the systematics of the measurement (e.g. normalization, beam energy) are the same for any experimental point and must not be evaluated at each energy step. However a precise determination of the angle of the hard photon as well as the full control of events with the photon emitted in the final state (pure QED FSR or other resonant processes, as for example $\phi \to \pi^+\pi^-\gamma$ [23]), is required.

2. Analysis of the process $e^+e^- \to \pi^+\pi^-\gamma$

Due to the importance of the 2π final state for a_μ^{had}, we concentrated at KLOE on the analysis of the radiative process $e^+e^- \to \pi^+\pi^-\gamma$, whose feasibility has been extensively studied by Monte Carlo [24].

2.1. The KLOE Detector

KLOE [25] is a typical e^+e^- multiple purpose detector with cylindrical geometry, consisting of a large helium based drift chamber (DC, [26]), surrounded by an electromagnetic calorimeter (EmC, [27]) and a superconducting magnet ($B = 0.52$ T). The detector has been designed for the measurement of CP violation in the neutral kaon system, i.e. for precise detection of the decay products of K_S and K_L. These are low momenta charged tracks ($\pi^\pm, \mu^\pm, e^\pm$ with a momentum range from 150 MeV/c to 270 MeV/c) and low energy photons (down to 20 MeV).

The DC dimensions (3.3 m length, 2 m radius), the drift cell shapes (2x2 cm^2 cells for the inner 12 layers, 3x3 cm^2 cells for the outer 46 layers) and the choice of the gas mixture (90% Helium, 10% Isobutane; $X_0 = 900$ m) had to be optimized for the requirements prevailing at a ϕ factory. The KLOE design results in a very good momentum resolution: $\sigma_{p_\perp}/p_\perp \leq 0.4\%$ at high tracking efficiencies ($> 99\%$).

The EmC is made of a matrix of scintillating fibres embedded in lead, which guarantees a good energy resolution $\sigma_E/E = 5.7\%/\sqrt{E(\text{GeV})}$ and excellent timing resolution

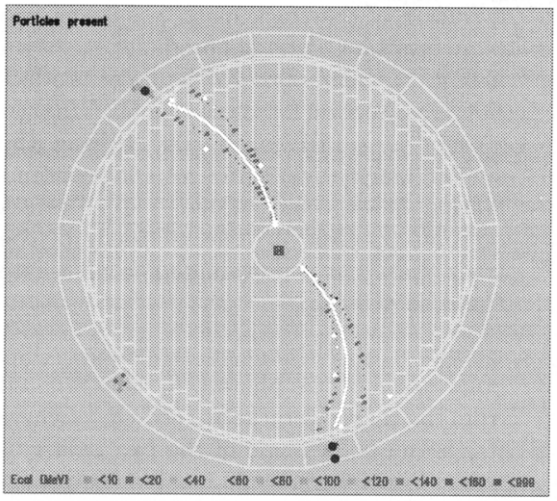

Figure 1. KLOE event display of a $\pi^+\pi^-\gamma$ event.

$\sigma_t = 57\text{ps}/\sqrt{E(\text{GeV})} \oplus 50$ ps. The EmC consists of a barrel and two endcaps which are surrounding the cylindrical DC; this gives a hermetic coverage of the solid angle (98%). However, the acceptance of the EmC below $\approx 20°$ is reduced due to the presence of quadrupole magnets close to the interaction point and does not allow to measure e.g. the photon of $\pi^+\pi^-\gamma$ events with low θ_γ angles.

It will be shown in the following that an efficient selection of the $\pi^+\pi^-\gamma$ signal is possible, without requiring an explicit photon detection. The relatively simple signature of the signal (2 high momentum tracks from the interaction point, see Fig. 1) and the good momentum resolution of the KLOE tracking detector allow us to perform such a selection.

2.2. Signal selection

The selection of $e^+e^- \to \pi^+\pi^-\gamma$ events is done in the following steps:

- *detection of two charged tracks*, with polar angle bewteen 40^o and 140^o, coming from a vertex in the fiducial volume $R < 8$ cm, $|z| < 15$ cm. The cuts on the transverse momentum $p_T > 200$ MeV or on the longitudinal momentum $|p_z| > 90$ MeV reject tracks spiralizing along the beam line, ensuring good reconstruction conditions. The probability to reconstruct a vertex in the drift chamber is $\sim 95\%$ and has been studied with Bhabha data, selected using the calorimeter only. The overall tracking reconstruction efficiency has been also evaluated using $\pi^+\pi^-\pi^0$ events selected by detecting π^0 in the electromagnetic calorimeter;
- *identification of pion tracks*: a Likelihood Method, using the time of flight of the particle and the shape of the energy deposit in the electromagnetic calorimeter, has been developed to reject the $e^+e^- \to e^+e^-\gamma$ background. A control sample of $\pi^+\pi^-\pi^0$ has been used to study the behaviour of pions in the electromagnetic calorimeter, since their interaction are not well reproduced by Monte Carlo. The effect of the selection on $\pi^+\pi^-\gamma$ and $e^+e^-\gamma$ events is visible in the upper plot of Fig. 2, as a function of the track mass, M_{track}: this variable is calculated from the reconstructed momenta, $\vec{p}_+$, $\vec{p}_-$, applying 4-momentum conservation, under the hypothesis that the final state consists of two particles with the same mass and one photon. For each event class ($\mu^+\mu^-\gamma$, $\pi^+\pi^-\gamma$) the track mass distribution is peaked at the proper mass; $\pi^+\pi^-\pi^0$ events populate the region on the right of the $\pi^+\pi^-\gamma$ peak. As it can be noted from Fig. 2, *up*, $e^+e^-\gamma$ events are drastically reduced, while the $\pi^+\pi^-\gamma$ peak is essentially unaffected by this selection (the estimated signal efficiency is larger than 98%).
- *cut on the track mass*: $\mu^+\mu^-\gamma$ events are rejected by a cut at 120 MeV in the track mass. The discrimination between π and μ using calorimeter information is not helpful since pions behave frequently like minimum ionizing particles. After this cut we find a contamination of $\mu^+\mu^-\gamma$ background smaller than 1%. $\pi^+\pi^-\pi^0$ events are rejected with a cut in the two-dimensional dis-

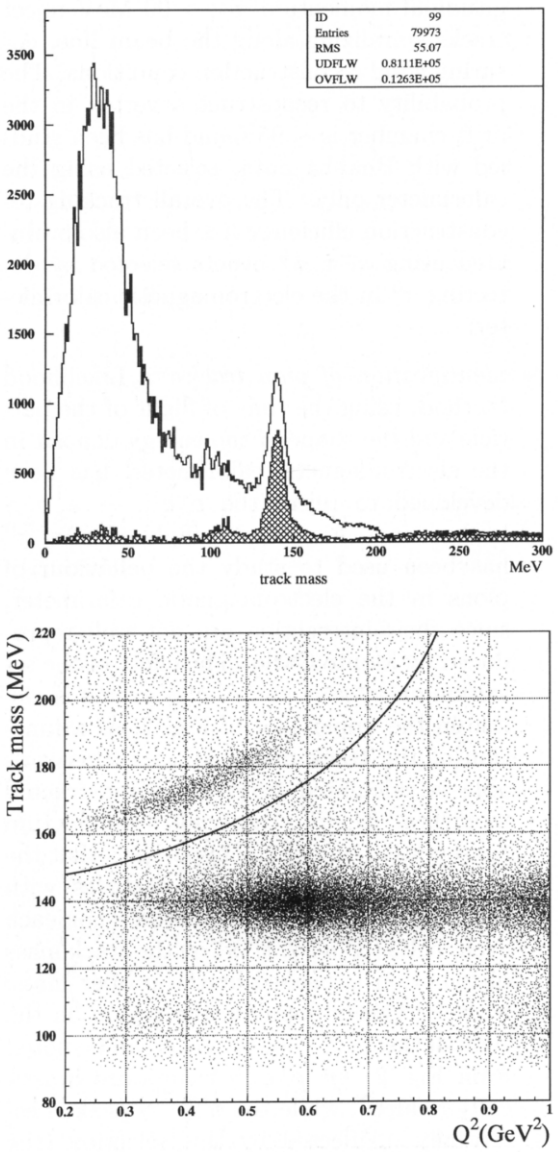

Figure 2. *Up*: track mass distribution before and after the likelihood selection. $\mu^+\mu^-\gamma$, $\pi^+\pi^-\gamma$ distributions are peaked at the proper mass, three pion events populate the region on the right of the $\pi^+\pi^-\gamma$ peak. *Down*: cut in the plane ($Q^2_{\pi\pi}$, track mass) used to reject $\pi^+\pi^-\pi^0$ events.

tribution of the track mass versus the two pion invariant mass squared, $Q^2_{\pi\pi}$, shown in Fig. 2, *down*. Due to the large production cross section for these events ($BR(\phi \to \pi^+\pi^-\pi^0) \sim 15\%$, $\sigma \sim 500$ nb) and the similar kinematics, some residual contamination is expected at small $Q^2_{\pi\pi}$ values ($Q^2_{\pi\pi} < 0.4\,GeV^2$). The efficiency of the track mass cut, as evaluated from Monte Carlo, is $\sim 90\%$;

- *definition of the angular acceptance:* The polar angle of the photon, θ_γ is calculated from the charged tracks as $180^0 - \theta_{\pi\pi}$, where $\theta_{\pi\pi}$ is the polar angle of the two pion system. Two fiducial volumes for the analysis of $\pi^+\pi^-\gamma$ events are defined: $\theta_\gamma < 15^o$ or $\theta_\gamma > 165^o$ (small angle analysis) and $55^o < \theta_\gamma < 125^o$ (large angle analysis). These two regions mainly differ for FSR and background contamination [28].

In this paper we will show the preliminary results obtained on the analysis at small angle ($\theta_\gamma < 15^o$ or $\theta_\gamma > 165^o$, $40^o < \theta_\pi < 140^o$).

3. Final State Radiation

It is now a common understanding that the radiation of one hard photon by final pions should be included in the measurement of the hadronic cross section for the evaluation of a_μ^{had} [29,2,30, 10,11].

However [14], in the case of radiative return, the differential cross section for the process $e^+e^- \to \pi^+\pi^-\gamma$ is proportional to the pion form factor squared at the measured $Q^2_{\pi\pi}$ only for ISR:

$$\left(\frac{d\sigma}{dQ^2}\right)_{ISR} \sim |F_\pi(Q^2)|^2 \sim \sigma_{e^+e^-\to\pi^+\pi^-}(Q^2), \quad (2)$$

while for FSR the differential cross section [2] is proportional to the pion form factor evaluated at the ϕ mass squared:

$$\left(\frac{d\sigma}{dQ^2}\right)_{FSR} \sim |F_\pi(M_\phi^2)|^2 \not= \sigma_{e^+e^-\to\pi^+\pi^-}(Q^2). \quad (3)$$

For this reason events due to FSR must be properly rejected by the analysis cuts.

[2] If no additional photons are emitted in the initial state.

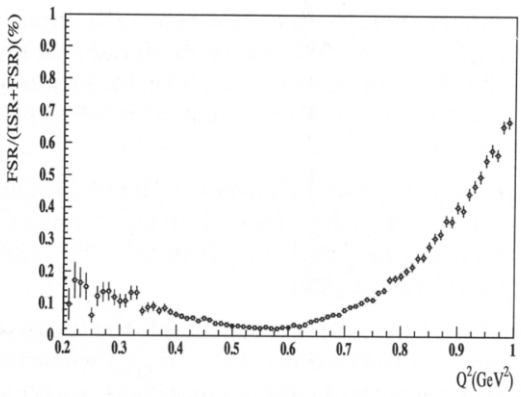

Figure 3. Ratio $FSR/(FSR+ISR)$ as a function of the two pions invariant mass for $\theta_\gamma < 15^o$ or $\theta_\gamma > 165^o$, $40^o < \theta_\pi < 140^o$.

Fig. 3 shows the ratio $FSR/(ISR+FSR)$ as a function of the $Q^2_{\pi\pi}$ for the small angle region ($\theta_\gamma < 15^o$ or $\theta_\gamma > 165^o$, $40^o < \theta_\pi < 140^o$). As it can be noted the average value of this ratio is below 0.5%.

4. Results

4.1. Effective cross section

Fig. 4 *up* shows the number of $\pi\pi\gamma$ events selected inside the small angle acceptance cuts at the end of the selection chain, for 100 bins between 0.02 and 1.02 GeV^2. This distribution corresponds to $\sim$ 73pb^{-1} of analyzed data out of $\sim 200\,pb^{-1}$ collected in 2001 and already reconstructed. More than 1083000 were selected, corresponding to 15000 events/pb^{-1}.

Even before unfolding the spectrum for the detector resolution effects, the $\rho - \omega$ interference (as well as the radiative tail) can be clearly seen, showing the excellent momentum resolution of the KLOE DC.

4.2. Pion form factor calculation

Neglecting FSR interference, the pion form factor can be extracted as a function of $Q^2_{\pi\pi}$, from

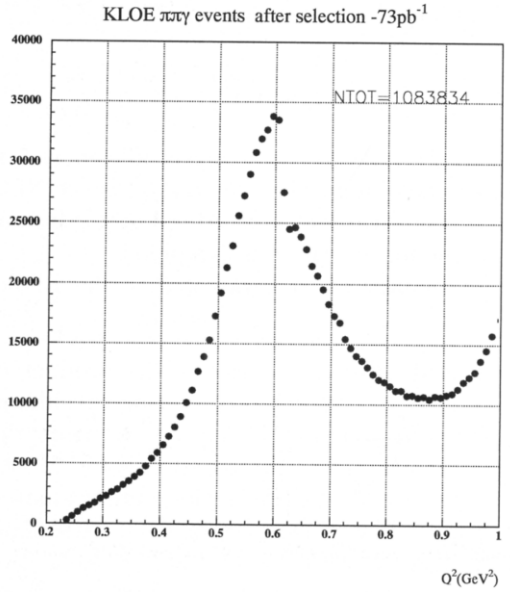

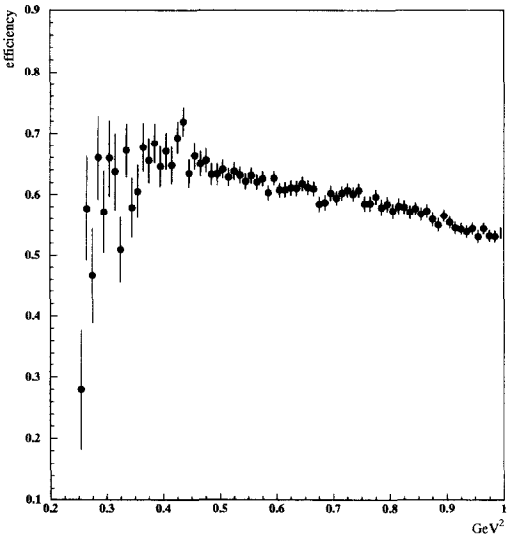

Figure 4. *Up*: Number of $\pi^+\pi^-\gamma$ events selected by the analysis in the region $\theta_\gamma < 15^o$ or $\theta_\gamma > 165^o$, $40^o < \theta_\pi < 140^o$. *Down*: Global efficiency as a function of $Q^2_{\pi\pi}$.

the observed $\pi^+\pi^-\gamma$ spectrum (N^{obs}) as:

$$|F_\pi(Q_i^2)|^2 = \frac{N_i^{obs}}{\epsilon(Q_i^2)LH(Q_i^2)} \quad (4)$$

where $\epsilon(Q_i^2)$ is the global analysis efficiency, L is the integrated luminosity and $H(Q_i^2)$ is the NLO cross section for $e^+e^- \to \pi^+\pi^-\gamma$ (only ISR) under the assumption of pointlike pions.

These quantities were evaluated in the following ways:

1. **global efficiency**: this is the product of trigger, reconstruction, filtering, likelihood and M_{track} cut efficiency. Apart from the latter which was evaluated only by Monte Carlo, the other efficiencies were evaluated from unbiased samples of data with similar kinematics (like $\pi^+\pi^-\pi^0$, Bhabha's or $\pi^+\pi^-\gamma$ itself). The Monte Carlo was used to generate the appropriate $\pi^+\pi^-\gamma$ phase space.

   Fig. 4, *down*, shows the dependence of the global efficiency as a function of reconstructed $Q^2_{\pi\pi}$ (only statistical errors are shown). Above $0.4\,GeV^2$ the average error is 2%, mainly dominated by the limited Monte Carlo statistics. Below $0.4\,GeV^2$ the error is larger, reflecting again the limited Monte Carlo statistics used in the evaluation of M_{track} cut efficiency.

2. **Luminosity**: The DAΦNE accelerator does not have luminosity monitors at small angle due to the existence of focusing quadrupole magnets very close to the interaction point. The luminosity is therefore measured using Large Angle Bhabhas ($55^o < \theta_{+,-} < 125^o$, $\sigma = 425$nb). The number of LAB candidates are counted and normalized to the effective Bhabha cross section obtained from Monte Carlo.

   The precision of this measurement depends both on the understanding of experimental efficiencies and acceptances and on the theoretical knowledge of the process.

   The systematic errors arising from the LAB selection cuts are well below 1%. All the selection efficiencies concerning the LAB measurement (Trigger, EmC clusters, DC tracking) are above 98% and well reproduced by the detector simulation. The background due to $\mu^+\mu^-\gamma$, $\pi^+\pi^-\gamma$ and $\pi^+\pi^-\pi^0$ is below 1%.

   KLOE uses two independent Bhabha event generators (the Berends/Kleiss generator [31] modified for DAΦNE [32] and BABAYAGA [33]).

   The very good agreement of the experimental distributions ($\theta_{+,-}$, $E_{+,-}$) with the event generators and a cross check with an independent luminosity counter based on $e^+e^- \to \gamma\gamma(\gamma)$ indicates a precision of better than 1%.

   More systematics checks (e.g. the effect of a varying beam energy and of a displaced beam interaction point) are under way.

3. **determination of H:** The NLO cross section for pointlike pions H was computed for each bin of $Q^2_{\pi\pi}$ using a modified version of PHOKHARA, in which $F_\pi(Q^2) = 1$.

   $2 \cdot 10^6$ events were generated within the acceptance of the small angle analysis: $\theta_\gamma < 15^o$ or $\theta_\gamma > 165^o$, $40^o < \theta_\pi < 140^o$. Fig. 5 shows a comparison between the differential cross section generated by Monte Carlo with a given parametrization of the pion form factor (*white dots*), and the same assuming pointlike pions (*black dots*).

   The systematical error on the numerical evaluation of H for the given acceptance cuts is estimated to be less than 1% by comparing the pion form factor obtained by dividing *bin-by-bin* the two distributions of Fig. 5 with the expected analytical parametrization.

The pion form factor extracted using eq. 4, is shown in Fig. 6. The spectrum can be divided in three regions according to the measurement error: below $0.4\,GeV^2$ with an error of 5-10%, between $0.4\,GeV^2$ and $0.5\,GeV^2$, with an average error of 3%, and above $0.5\,GeV^2$ with an average error of 2%. The measurement error is dominated by the

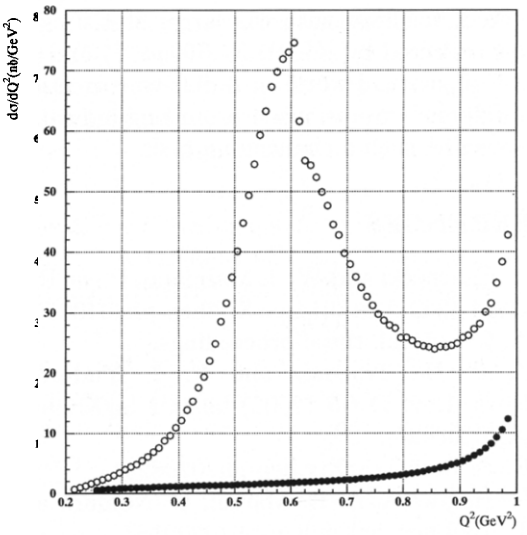

Figure 5. Differential $\pi^+\pi^-\gamma$ NLO cross section from Monte Carlo, for a given $F_\pi(Q^2)$ parametrization (*white dots*), and assuming pointlike pions, *i.e.* $F_\pi(Q^2) = 1$ (*black dots*). The cuts are $\theta_\gamma < 15^o$ or $\theta_\gamma > 165^o$, $40^o < \theta_\pi < 140^o$.

limited Monte Carlo statistics used in the evaluation of the efficiencies.

4.3. Fit of the pion form factor

A preliminary fit was applied to data using the parametrization for $F_\pi(Q^2)$ found in [34] (KS):

$$F_\pi(Q^2) = \frac{BW_\rho \frac{(1+\alpha BW_\omega)}{1+\alpha} + \beta BW_{\rho'}}{1+\beta} \qquad (5)$$

The mass and the width of the ρ as well as α and β were free parameters of the fit, while the other paramaters were kept fixed (to the values of [11]).

The results obtained from the fit were: $M_\rho = (772.6 \pm 0.5)\,MeV$, $\Gamma_\rho = (143.7 \pm 0.7)\,MeV$, $\alpha = (1.48 \pm 0.12) \cdot 10^{-3}$, $\beta = -0.147 \pm 0.002$. These values, even if preliminary, are in good agreement with the ones found by CMD-2 [11] using a light different parametrization (Gounaris-

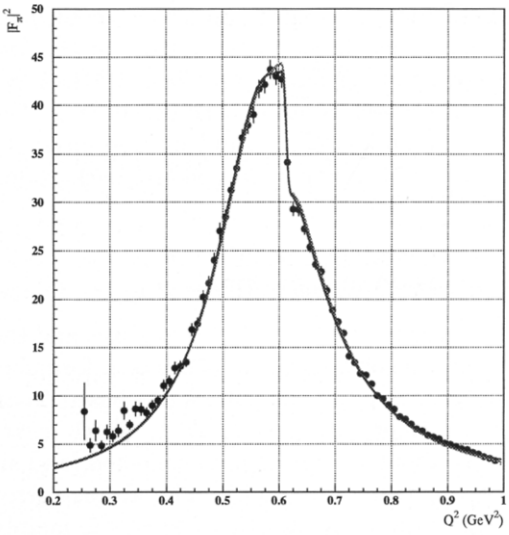

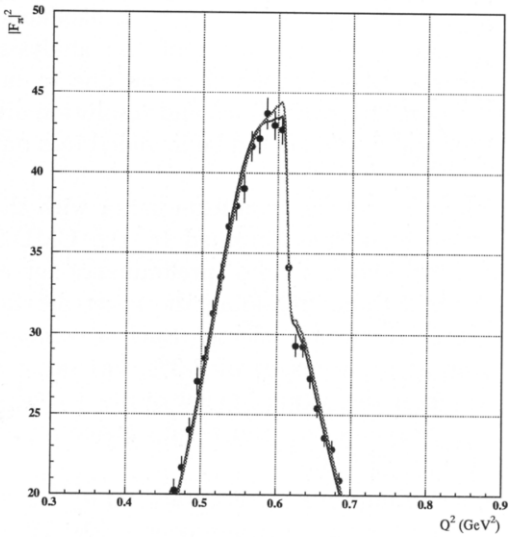

Figure 6. *Up*: Preliminary measurement of the pion form factor. Overimposed are the analytical $|F_\pi(Q^2)|^2$ parametrizations, obtained by a fit to the KLOE data using KS model (*blue line*), and the parametrization found from CMD-2 with the GS model (*red line*). The two curves are very similar. *Down*: zoom of $|F_\pi(Q^2)|^2$ around the ρ peak. The *blue line* is obtained by a fit to the KLOE data using KS model, while the *red* one is the parametrization found from CMD-2.

Sakurai). This agreement can be also confirmed from Fig. 6, which shows the results of the two parametrization (KLOE *blue line*, CMD-2 *red line*) overimposed to our experimental data. The discrepancy at low $Q^2_{\pi\pi}$ could be due either to the model inadequacy or to residual background events.

5. Conclusion and outlook

The status of $e^+e^- \to \pi^+\pi^-\gamma$ analysis and the preliminary results obtained on the pion form factor were presented. The analysis was based on an integrated luminosity of $\sim 73\,pb^{-1}$, which corresponds to about 1/3 of the data collected (and already reconstructed) in 2001. The average error for single point above $0.4\,GeV^2$ is $\sim 2\%$, mainly dominated by the the limited Monte Carlo statistics in the efficiency evaluation. FSR and other background channels (as for example Bhabha's or $\pi^+\pi^-\pi^0$) are kept below 1% by a likelihood method and kinematical cuts of the analysis. Other sources of systematical errors due to luminosity, radiative corrections and resolution are still under study, and should be included into our errors.

A comparison of the pion form factor with the fitted parametrization obtained by the CMD-2 collaboration, shows a good (preliminary) agreement, even without unfolding the spectrum for the detector resolution effects. Such a comparison, even at an accuracy of 2-3%, has become more and more important in view of the $1.6\,\sigma$ discrepancy between e^+e^- and τ data in the recent evaluation of a_μ^{had} [8].

In order to improve the accuracy on a_μ^{had} a final precision for this measurement below 1% is needed. This is very important both in the energy region around the ρ, where the CMD-2 collaboration has recently reached a 0.6% accuracy as well as below $0.6\,GeV$, which contributes to a_μ with about 100×10^{-10} and is known with a worse accuracy [10]. KLOE can study both these regions using $\pi^+\pi^-\gamma$ events with the hard photon emitted at small and large angle. However in order to reach such an highly demanding accuracy many factors must be well under control, both experimentally and theoretically. The results here presented, together with the larger statistics up to now collected by KLOE ($\sim 500\,pb^{-1}$) and the intense theoretical work on radiative corrections from different groups, are a promising indication for achieving such a challenging task.

REFERENCES

1. A. Czarnecki and W. J. Marciano, Phys. Rev. D **64** (2001) 013014 [arXiv:hep-ph/0102122]; A. Czarnecki, these proceedings.
2. J. F. De Troconiz and F. J. Yndurain, Phys. Rev. D **65** (2002) 093001 [arXiv:hep-ph/0106025].
3. E. de Rafael, arXiv:hep-ph/0208251.
4. K. Hagiwara, A. D. Martin, D. Nomura and T. Teubner, arXiv:hep-ph/0209187.
5. G. W. Bennett *et al.* [Muon g-2 Collaboration], Phys. Rev. Lett. **89** (2002) 101804 [Erratum-ibid. **89** (2002) 129903] [arXiv:hep-ex/0208001]; L. Roberts, these proceedings.
6. F. Jegerlehner, arXiv:hep-ph/0104304.
7. M. Davier and A. Höcker, Phys. Lett. B **435** (1998) 427 [arXiv:hep-ph/9805470].
8. M. Davier, S. Eidelman, A. Höcker and Z. Zhang, arXiv:hep-ph/0208177; A. Höcker, these proceedings.
9. M. Davier, these proceedings.
10. S. Eidelman, these proceedings.
11. R. R. Akhmetshin *et al.* [CMD-2 Collaboration], Phys. Lett. B **527** (2002) 161 [arXiv:hep-ex/0112031].
12. S. Guiducci *et al*, Proceedings of PAC99, New York, March 1999.
13. S. Spagnolo, Eur. Phys. J. C **6** (1999) 637.
14. S. Binner, J. H. Kühn and K. Melnikov, Phys. Lett. B **459** (1999) 279 [arXiv:hep-ph/9902399].
15. A. B. Arbuzov, E. A. Kuraev, N. P. Merenkov and L. Trentadue, JHEP **9812** (1998) 009 [arXiv:hep-ph/9804430].
16. M. I. Konchatnij and N. P. Merenkov, JETP Lett. **69** (1999) 811 [arXiv:hep-ph/9903383].
17. V. A. Khoze, M. I. Konchatnij, N. P. Merenkov, G. Pancheri, L. Trentadue and O. N. Shekhovzova, Eur. Phys. J. C **18** (2001) 481 [arXiv:hep-ph/0003313].
18. V. A. Khoze, M. I. Konchatnij,

N. P. Merenkov, G. Pancheri, L. Trentadue and O. N. Shekhovtzova, Eur. Phys. J. C **25**, 199 (2002) [arXiv:hep-ph/0202021].
19. G. Rodrigo, H. Czyz, J. H. Kühn and M. Szopa, Eur. Phys. J. C **24** (2002) 71 [arXiv:hep-ph/0112184].
20. J. H. Kühn and G. Rodrigo, Eur. Phys. J. C **25** (2002) 215 [arXiv:hep-ph/0204283].
21. G. Rodrigo, H. Czyz and J. H. Kühn, arXiv:hep-ph/0205097.
22. , G. Rodrigo, these proceedings.
23. K. Melnikov, F. Nguyen, B. Valeriani and G. Venanzoni, Phys. Lett. B **477**, 114 (2000) [arXiv:hep-ph/0001064].
24. G. Cataldi, A. Denig, W. Kluge, S. Müller and G. Venanzoni, *Published in Frascati 1999, Physics and detectors for DAPHNE* 569-578*
25. A. Aloisio *et al.* [KLOE Collaboration], LNF-93-002-IR.
26. M. Adinolfi *et al.*, Nucl. Instrum. Meth. A **488** (2002) 51.
27. M. Adinolfi *et al.*, Nucl. Instrum. Meth. A **482** (2002) 364.
28. B. Valeriani *et al.* [KLOE Collaboration], arXiv:hep-ex/0205046.
29. K. Melnikov, Int. J. Mod. Phys. A **16** (2001) 4591 [arXiv:hep-ph/0105267].
30. A. Hoefer, J. Gluza and F. Jegerlehner, Eur. Phys. J. C **24** (2002) 51 [arXiv:hep-ph/0107154].
31. F. A. Berends and R. Kleiss, Nucl. Phys. B **228** (1983) 537.
32. E. Drago and G. Venanzoni, INFN-AE-97-48.
33. C. M. Carloni Calame, C. Lunardini, G. Montagna, O. Nicrosini and F. Piccinini, Nucl. Phys. B **584** (2000) 459 [arXiv:hep-ph/0003268].
34. J. H. Kühn and A. Santamaria, Z. Phys. C **48** (1990) 445.